Performance Analysis of the Circular Folding Cooperative Power Spectral Density Split Cancellation Algorithm for Spectrum Sensing Under Errors at the Quantized Report Channel

Eduardo M. de Almeida*, Lucas dos S. Costa*, Rausley A. A. de Souza*, and Dayan A. Guimarães*
*National Institute of Telecommunications, Inatel, Santa Rita do Sapucaí - MG - Brazil
Email: {lucass,rausley,dayan}@inatel.br, eduardo_telecom@hotmail.com

***Abstract*—The circular folding cooperative power spectral density split cancellation (CF-CPSC) algorithm was recently proposed for detecting idle bands in centralized cooperative spectrum sensing for cognitive radio (CR) applications. This algorithm has low complexity and is robust under nonuniform noise. This paper analyzes the performance of the CF-CPSC under quantized and erroneous report channel transmissions. Two approaches has been investigated regarding the CF-CPSC test statistic: i) it is completely computed at the fusion center (FC), and ii) it is partially calculated at each CR for saving report channel resources. In both cases, the information to be reported by the CRs are uniformly quantized and then submitted to errors. Results show that the CF-CPSC is also robust to the quantization and report errors. The second approach is more sensitive to the quantization and report channel errors, but less channel resources are used in comparison with the first approach. The smaller resource usage is achieved by the second approach even with error correcting codes, which increases the amount of data through the report channel. The resource usage achieved by the first approach is larger, even with no error correcting codes.**

I. Introduction

The radio frequency resources have becoming unavailable as a consequence of the rapid growth of the wireless communication services in the past few years. This unavailability is mainly due to the advent of the Internet of things (IoT) and the fifth generation (5G) of wireless communication systems, which predict spectrum allocation to a huge amount of wireless devices [1]. Seeking for a solution to this problem, researchers and spectrum allocation regulatory bodies, like the Federal Communication Commission (FCC), discovered that the spectrum bands are actually underutilized in some areas [2]. It was found that the primary users (PUs), which are the spectrum owners, do not transmit information uninterruptedly, leaving vacant bands during some periods. This discovery was viewed as an opportunity to provide better use of the spectrum and drove the efforts to the creation of new spectrum management policies for more efficient utilization of this resource.

The earlier concept of spectrum allocation policy is based on the grant of exclusive use by the PUs, also known as licensed users, in some location and for the negotiated period of time. The recently admitted new spectrum allocation policy, however, gives chances to unlicensed users, or secondary users (SUs), to use portions of the spectrum to transmit their information, if they find idle bands.

The cognitive radio (CR) concept emerged from this idea to give cognition capability to the SUs to sense the spectrum and find idle bands for opportunistic access. The task of sensing the spectrum [3] is one of the most important tasks of a CR and can be performed cooperatively with other CRs (the cooperative spectrum sensing), or not (the non cooperative spectrum sensing). In the non cooperative approach, a CR is autonomous in the task of sensing and making the final decision on the occupancy of the sensed channel. The cooperative spectrum sensing is more reliable, since a group of CRs cooperate with each other to reach a less erroneous decision. The cooperation can overcome detrimental effects like the multipath fading, the shadowing and the hidden node problems.

In centralized cooperative spectrum sensing, each cooperating device shares its sensing information with a central node, called fusion center (FC), for combination and final decision, and to control the CRs activity. This final decision is achieved by forming a test statistic based on some spectrum sensing detection technique. The most common are the energy detection (ED), the matched filter detection (MFD), the cycloestationary feature detection (CFD) and those based on the eigenvalues of the received signal covariance matrix [4], [5]. In this last group it can be mentioned the generalized likelihood ratio test (GLRT), the maximum-minimum eigenvalue detection (MMED), and the maximum eigenvalue detection (MED).

The type of information sent by the CRs to the FC, e.g., individual decisions, samples, eigenvalues, etc., defines two kinds of fusion: the hard decision and the soft (data) decision fusion. The hard decision fusion is the one in which each cooperating device computes a given test statistic to sense

This work was supported in part by CNPq under Grant 308365/2017-8, and in part by Finep (with Funttel resources) Grant 01.14.0231.00, under the Radiocommunications Reference Center (CRR) project of the National Institute of Telecommunications (Inatel), Brazil.

978-1-5386-6754-5/18/$31.00 ©2018 IEEE

the targeted band, makes a local decision on the occupation state of this band, and sends the decision to the FC. The FC combines the CRs decisions, makes the final decision and informs it back to the CRs to grant, or not, access to the spectrum. The soft (data) decision fusion is the one in which the test statistic is fully or partially, computed at the FC. In this case, each CR collects samples of the received signal and sends these samples or some processed version of them to the FC, where the final test statistic is formed for subsequent final decision.

This paper adopts the circular folding cooperative power spectral density split cancellation (CF-CPSC) algorithm [6] as the spectrum sensing technique, since it has low implementation complexity and is robust under nonuniform noise, a situation in which each cooperating CR operates under different noise variances. Besides, the authors of [6] showed that the CF-CPSC outperforms its predecessor, the cooperative power spectral density split cancellation (CPSC), and the GLRT, under shadowed-fading and frequency selective sensing channels. However, the report channel in [6] was assumed to be ideal, not producing any error in the information transmitted to the FC.

This paper addresses the same scenario of [6] in terms of shadowed-fading and frequency selective sensing channels, additionally adopting imperfect report channels. Moreover, the CF-CPSC algorithm is assumed to be fully computed at the FC, an approach in which the CRs sense the targeted band and just send the received samples to the FC for processing, as well as partially computed at the CRs, aiming at reducing the volume of data through the report channel. In the latter approach, only part of the CF-CPSC algorithm is computed by the CRs. The CRs then send the partial results to the FC, where the algorithm is completed and the final test statistic is formed. This paper also analyses the influence of the uniform quantization error and the uniform quantization error plus bit error with and without error correcting codes at the report channel on the spectrum sensing performance, as these effects are intrinsically present in many digital communication processes.

The CF-CPSC performances are assessed under various system parameters in both of the above-described approaches. Results show that it is robust anyway and, although more susceptible to bit and quantization errors at the report channel when the algorithm is partially computed at each CR, the loss in performance can be overcome with a simple repetition code, yet keeping the data traffic smaller than when the algorithm is fully computed at the FC with no error correcting codes.

The remainder of the paper follows this introductory section by presenting the system model in Section II (including both CF-CPSC algorithmic approaches, the uniform quantization, the report channel errors and the repetition encoding). Numerical results are given in Section III and the conclusions are drawn in Section IV.

II. System Model

The process of sensing and making a decision on the presence or absence of the PU signal in a target band can be described as a binary hypothesis test [7]: $x_u(n) = \{\sum_{z=0}^{Z-1} h_u(z)s(n-z) + w_u(n) \mid \mathcal{H}_1\}$ or $x_u(n) = \{w_u(n) \mid \mathcal{H}_0\}$, where $x_u(n)$ represents the received signal at the u-th CR, $u = 1, 2, \ldots, U$, $w_u(n)$ corresponds to the n-th sample of a zero mean circularly-symmetric additive white Gaussian noise (AWGN) with standard deviation σ_w at the u-th CR, $n = 1, 2, \ldots, N$, and $h_u(n)$ is a Z-tap time-varying impulse response of the channel between the PU and the u-th CR. This impulse response models a frequency-selective and slow shadowed-fading sensing channel [6]. The hypotheses $\mathcal{H}_0$ and $\mathcal{H}_1$ respectively denote the absence and the presence of the PU signal in the sensed band. Under $\mathcal{H}_1$, the unknown and deterministic PU signal $s(n)$ is convolved with the unknown impulse response $h_u(n)$.

A. CF-CPSC Algorithm

Following [6], the steps of the CF-CPSC algorithm are:
1) Calculate the instantaneous received signal power spectral density (PSD) at the u-th CR,

$$F'_u(n) = \tfrac{1}{N}|\mathrm{DFT}\{x_u(n)\}|^2, \tag{1}$$

where $\mathrm{DFT}\{\cdot\}$ is the discrete Fourier transform (DFT).
2) Find the modified circular-even component of $F'_u(n)$ as

$$F_u[k] = \begin{cases} \frac{F'_u[1]+F'_u[N/2+1]}{2}, & k=1, \\ \frac{F'_u[k]+F'_u[N-k+2]}{2}, & k=2,3,\ldots,N. \end{cases} \tag{2}$$

3) Split the bandwidth sensed by the u-th CR into L sub-bands, each one having $V = N/(2L)$ samples, and compute the signal power into the ℓ-th, $\ell = 1, 2, \ldots, L$, sub-band as

$$F_{\ell_u} = \sum_{k=1}^{V} F_u\left[(\ell-1)\,V + k\right]. \tag{3}$$

4) Compute the total received signal power in the overall bandwidth sensed by the u-th CR, according to

$$F_{\mathrm{full}_u} = \sum_{k=1}^{N/2} F_u[k]. \tag{4}$$

5) Compute the ratio between the ℓ-th sub-band signal power and the total received signal power for the u-th CR as

$$r_{u,\ell} = F_{\ell_u}/F_{\mathrm{full}_u}, \tag{5}$$

which cancels-out the noise variance. These ratios are the test statistic for each sub-band at the u-th CR.
6) Average $r_{u,\ell}$ over all CRs to obtain a combined statistic for the ℓ-th sub-band, according to

$$r_{\mathrm{avr}}(\ell) = \tfrac{1}{U}\sum_{u=1}^{U} r_{u,\ell}. \tag{6}$$

7) Compare the ℓ-th average with the predefined *global* decision threshold γ at the FC to make a decision upon each sub-band as

$$\begin{cases} r_{\mathrm{avr}}(\ell) < \gamma, & \text{decide } \mathcal{H}_0 \text{ for } \ell\text{-th sub-band} \\ r_{\mathrm{avr}}(\ell) \geq \gamma, & \text{decide } \mathcal{H}_1 \text{ for } \ell\text{-th sub-band} \end{cases}. \tag{7}$$

8) Make a final decision on the occupation state of the sensed PU channel according to

$$\begin{cases} \text{All sub-bands decided } \mathcal{H}_0, & \text{decide } \mathcal{H}_0 \\ \text{One or more sub-bands decided } \mathcal{H}_1, & \text{decide } \mathcal{H}_1 \end{cases}. \quad (8)$$

It is worthy emphasizing that all the steps were originally meant to be executed at the FC, which corresponds to the first approach previously mentioned. For the other approach, the algorithm is partially computed by the CRs, up to the Step 5, from which the ratios $r_{u,\ell}$ in (5) are obtained. These ratios are then sent by the CRs to the FC, where the remaining steps are computed for final test statistic calculation. In this second approach, considerable report channel resources can be saved, but at the cost of a larger processing capacity that must be shifted from the FC to the CRs.

B. Uniform Quantization

A b-bit uniform quantization can be described as a process of discretizing some analog signal into $Q = 2^b$ equally spaced quantization levels, yielding $Q - 1$ decision levels and Q adjacent quantization regions having equal width. As depicted in Fig. 1, the quantizer output levels are $\{n_1, n_2, \ldots, n_Q\}$, the decision levels are $\{z_1, z_2, \ldots, z_{Q-1}\}$, and the quantization regions are

$$r_i = \begin{cases} (\xi, z_i], & i = 1 \\ [z_{i-1}, z_i], & 2 \leq i \leq Q-1, \\ [z_{i-1}, +\infty), & i = Q \end{cases} \quad (9)$$

where $\xi = 0$ for an unsigned uniform quantizer and $\xi = -\infty$ for a signed uniform quantizer.

Taking into account signed and unsigned fixed point operation uniform quantizers [8], the output levels can be written as $n_i = n_1 + Sl$, $l = 0, 1, \ldots, N_Q - 1$, and the decision levels as $z_i = (n_i + n_{i+1})/2$, $1 \leq i < Q$. The variable $S = 2^{-f}$ is a scaling factor and $f = 0, 1, \ldots, b$ is the number of bits determining the resolution of the fractional part of the output levels n_i. For the signed quantizer, the minimum output level is $n_1 = -S(2^{b-1})$, for $l = 0$, and the maximum is $n_Q = S(2^{b-1} - 1)$, for $l = Q - 1$. Notice that the output levels are not symmetric about $n_{Q/2+1}$. In this case, $n_{Q/2+1} = 0$ and $|n_1| > n_Q$. For the unsigned quantizer, $n_1 = 0$ for $l = 0$, $n_{Q/2+1} = S(2^b/2)$, with $l = Q/2$ and $n_Q = S(2^{b-1})$ for $l = Q - 1$.

The above quantizers are used in both approaches studied in this paper: the **Approach 1** assumes that the CF-CPSC algorithm is fully computed at the FC. For the **Approach 2**, the CF-CPSC algorithm is partially executed in each CR and partially at the FC. These approaches are detailed in the sequel, where $[\cdot]^{(b)}$ means that the generic quantity inside brackets is quantized with b bits.

*1) **Approach 1**:* The samples $x_u(n)$ collected by the u-th CR are firstly normalized with respect to the quantized maximum absolute value $[\psi_u]^{(b)}$, yielding $x_u^{\mathrm{n}}(n) = x_u(n)/[\psi_u]^{(b)}$, with $[\psi_u]^{(b)} = \max\{\max\{|\Re[x_u(n)]|\}, \max\{|\Im[x_u(n)]|\}\}^{(3)}$, where $b = 3$ was chosen so that the spectrum sensing performance did not change with respect to the infinite quantization of ψ_u. Notice that $\{-1 \lessapprox x_u^{\mathrm{n}}(n) \lessapprox 1\}$. It must be emphasized that ψ_u is uniformly quantized by an unsigned quantizer, since it belongs to $\mathbb{R}^+$. Subsequently, $x_u^{\mathrm{n}}(n)$ is weighted by the maximum output value of a signed quantizer to fit the data into the dynamic range of the quantizer, yielding $x_u^{\mathrm{nw}}(n) = x_u^{\mathrm{n}}(n) n_Q$. This results in $\{-S(2^{b-1} - 1) \lessapprox x_u^{\mathrm{nw}}(n) \lessapprox S(2^{b-1} - 1)\}$, with $b = b_1$ to denote the use of the signed quantizer. Then, $[\psi_u]^{(3)}$ and $[x_u^{\mathrm{nw}}(n)]^{(b_1)}$ are sent to the FC.

After receiving the bits sent by the CRs, the FC tries to recover $[x_u(n)]^{(b_1)}$ through the following operation: $[x_u(n)]^{(b_1)} = [x_u^{\mathrm{nw}}(n)]^{(b_1)} [\psi_u]^{(3)} / n_Q$. Notice that the received bits possibly corrupted by the report channel will probably make $[x_u^{\mathrm{nw}}(n)]^{(b_1)}$ different from the corresponding quantities generated by the CRs, resulting in a corrupted $[x_u(n)]^{(b_1)}$. From $[x_u(n)]^{(b_1)}$, the FC applies the CF-CPSC algorithm from Step 1 to Step 8 in order to decide whether the sensed channel is under the $\mathcal{H}_1$ or under the $\mathcal{H}_0$ hypothesis.

*2) **Approach 2**:* The steps 1 to 5 of the CF-CPSC algorithm are performed by each CR, up to the computation of $r_{u,\ell}$. By the definition of (5), it follows that $0 < r_{u,\ell} < 1$. Then, there is no need for normalizing or weighting it before quantization, which now is made by an unsigned quantizer with $b = b_2$ bits. The resultant $[r_{u,\ell}]^{(b_2)}$ is the quantity transmitted over the report channel. The FC receives $[r_{u,\ell}]^{(b_2)}$, possibly corrupted by the report channel, and computes the steps 6 to 8 of the CF-CPSC algorithm in order to decide whether the sensed channel is under the hypothesis $\mathcal{H}_1$ or $\mathcal{H}_0$.

C. Control Channel Errors

In practice, it is mandatory to consider that bit errors will occur through the report channel, since this is an intrinsic characteristic of any communication channel. In this paper, the report channel errors are produced by passing the digitized data, i.e. $[x_u^{\mathrm{nw}}(n)]^{(b_1)}$, $[\psi_u]^{(3)}$ and $[r_{u,\ell}]^{(b_2)}$, through a memoryless binary symmetric channel (BSC), with a configurable crossover (error) probability P_{e}. In spite of being simple, this channel model can fairly mimic the modulation-channel-demodulation chain.

D. Repetition Code

The repetition code is used to protect the digitized data from the report channel errors. Although it is a trivial code (does not produce coding gain), it can bring diversity gain when applied to actual report channels with shadowing and fading, and suffices for the present analysis. The variables $[x_u^{\mathrm{nw}}(n)]^{(b_1)}$, $[\psi_u]^{(3)}$ and $[r_{u,\ell}]^{(b_2)}$ are encoded with configurable coding rate, $\bar{r} = 1/\bar{n}$, odd $\bar{n}$, where $\bar{n}$ is the coded block length. The coded bits received at the FC are decoded via majority rule, and the resultant bits go through a digital-to-analog conversion to produce the estimates of $[x_u(n)]^{(b_1)}$, $[\psi_u]^{(3)}$ and $[r_{u,\ell}]^{(b_2)}$. These estimates are then used by the FC to build the final CF-CPSC test statistic and decision upon the presence or absence of the PU signal in the sensed band.

III. Numerical Results

The simulation results presented hereafter were generated under the system parameters adopted in [6]. It is assumed

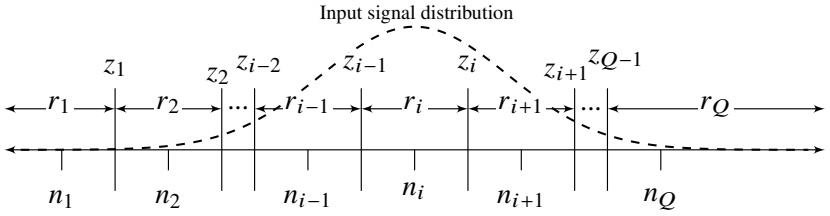

Fig. 1: Quantization levels, decision levels and decision regions of a uniform quantizer.

$U = 6$ cooperating CRs, with one antenna each. A single PU is adopted, with quaternary phase-shift keying (QPSK) transmitted signal generated in baseband with 4 samples per symbol. The sensing interval corresponds to 40 symbols, leading to $N = 160$ samples collected by each CR in each sensing interval. The number of sub-bands is $L = 5$, and the shadowed-fading sensing channel tap gains in $h_u(n)$ are log-normal combined with Rayleigh fading. The number of taps in $h_u(n)$ is $Z = 6$, following an outdoor negative exponential shape with average tap gains $[1, 0.447, 0.178, 0.079, 0.063, 0.112]$. The sensing channel gains are fixed during each sensing interval, but independent between sensing rounds. Moreover, these gains are independent for each CR and sensing channel tap. The shadowing is simulated with correlation among the CRs and is independent across the sensing rounds, with standard deviation of 4 dB, and with correlation level set according to a decorrelation distance [9] of 30 meters. The average signal-to-noise ratio (SNR) is -10 dB to comply with the predicted low SNR regime for spectrum sensing [10]. The noise powers at the input of the CRs are unequal, given by $[0.8, 0.9, 0.95, 1.1, 0.85, 1.15]$ watts.

Recalling that f is the number of quantization bits associated to the fractional part of the quantizer's output values under fixed point operation, the samples transmitted to the FC are quantized with $b_1 = f = 5$ bits under **Approach 1**, with ψ_u being quantized by 3 bits and $f = 1$. For the **Approach 2**, $r_{u,\ell}$ is quantized with $b_2 = f = 6$ bits. Taking into account that $\{-1 < [x_u(n)]^{(b_1)} < 1\}$, and that typically $\psi_u > 1$ and $r_{u,\ell} < 1$, the chosen values for f are justified.

The BSC crossover probabilities are $P_e = \{0, 10^{-2}, 5 \times 10^{-2}, 10^{-1}\}$. The repetition code rates are $\bar{r} = \{1, 1/3, 1/5, \ldots, 1/15\}$, where $\bar{r} = 1$ means that no channel encoding is produced.

The spectrum sensing performance is commonly assessed through the probability of false alarm, P_{fa}, and the probability of detection, P_d. The former is the probability of a final decision in favor of the presence of the PU signal, when actually the sensed channel is vacant. The latter is the probability of a decision in favor of the presence of the PU signal, when indeed this signal is present in the sensed band. These metrics are often evaluated through receiver operating characteristic (ROC) curves, which relates P_{fa} and P_d as the decision threshold is varied.

In this paper, each ROC point results from 50,000 Monte Carlo events, with the PU activity simulated as a Bernoulli random variable with 50% of the time in the *on* state, for detection rate computations, and 50% of the time in the *off* state, for false alarm rate computations. All the results were obtained with the MATLAB® software.

Figure 2 shows some ROCs of the CF-CPSC under quantization errors over the error free report channel ($P_e = 0$), as well as and under quantization errors over the erroneous report channel ($P_e > 0$), with ($\bar{r} < 1$) and without ($\bar{r} = 1$) channel encoding, for **Approach 1** (samples are quantized by $b_1 = 5$ bits and ψ_u is quantized with 3 bits), and for **Approach 2** ($r_{u,\ell}$ is quantized by $b_2 = 6$ bits). It was also included a raw data ROC, which considers no quantization error (infinite resolution granted by floating-point operations). This figure reveals that **Approach 2** is more sensitive to quantization errors than **Approach 1**, since the former needed $b_2 = 6$ bits, against $b_1 = 5$ in the latter, to achieve approximately the same performance achieved with the raw data. One can also notice that **Approach 2** is clearly more sensitive to channel errors than **Approach 1**, which can be seen by comparing the ROCs with $P_e > 0$ and $\bar{r} = 1$ in both approaches. Thus, a larger error correction capacity is needed for the channel code used under **Approach 2** to make the report transmissions practically immune to the produced errors. For instance, it was needed $\bar{r} = 1/3$, when $P_e = 10^{-2}$, in order to satisfactorily protect the report channel transmission in the **Approach 1**, while for the **Approach 2** $\bar{r} = 1/5$ was required. The same conclusions hold for the remaining values of $P_e > 0$. As a general conclusion, one can infer from Fig. 2 that the CF-CPSC is actually robust against channel errors, taking into consideration the high BSC crossover error probabilities adopted.

To emphasize the larger sensitivity of the **Approach 2** to quantization errors, Fig. 3 shows the area under the ROC curve (AUC) as a function of the number of quantization bits (b_1 or b_2, depending on the approach in analysis), considering no channel coding and error-free report channel ($P_e = 0$). The AUC for the raw data, which is not dependent on b_1 or b_2, is also available in Fig. 2 for comparisons. It can be seen that, with 2 quantization bits, the AUCs correspond to 0.87, 0.78 and 0.55 for the raw data, the **Approach 1** and the **Approach 2**, respectively. Notice that the performance of the **Approach 2** was severally degraded. It is worth emphasizing that this figure reveals the appropriateness of the number of bits $b_1 = 5$ used to quantize the samples in the **Approach 1**, and $b_2 = 6$ for the quantization of $r_{u,\ell}$ in the **Approach 2**, since their AUCs converge to the raw data AUC at these numbers of bits.

Figure 4 emphasizes the larger sensitivity of the **Approach 2** (dashed lines) to report channel errors, with and

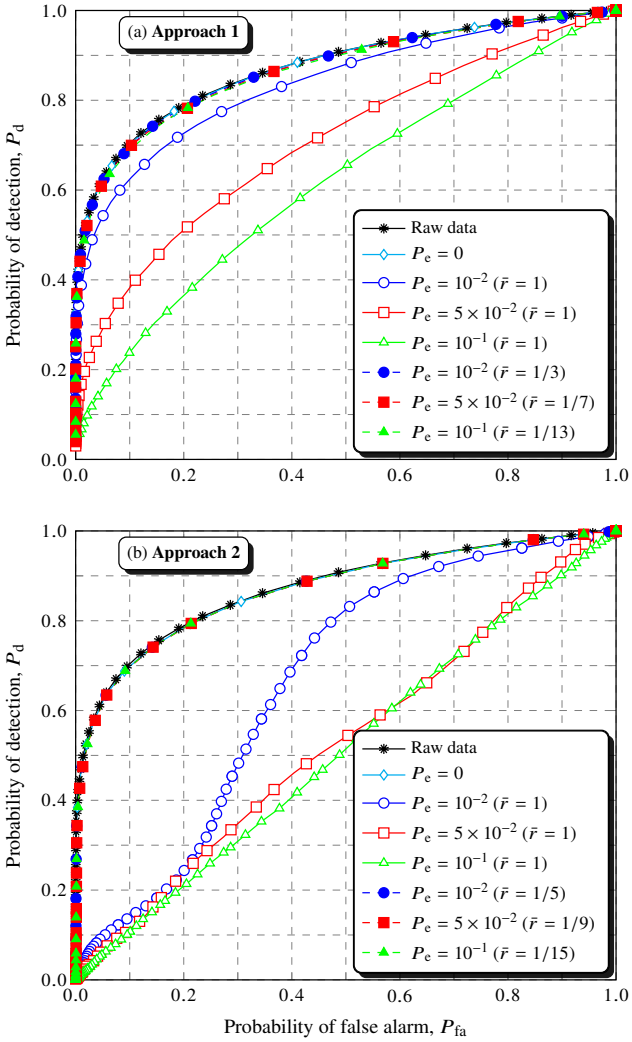

Fig. 2: ROCs for the CF-CPSC under **Approach 1** (a) and **Approach 2** (b), with quantization errors and with quantization errors plus bit errors, with and without error correcting code, for various values of P_e and $\bar{r}$. This figure is better viewed in color.

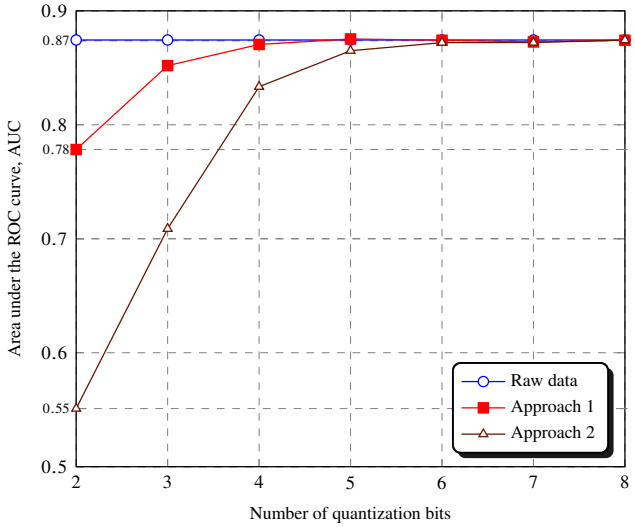

Fig. 3: AUC of the CF-CPSC as a function of the total number of quantization bits, with $P_e = 0$ and $\bar{r} = 1$, considering the **Approach 1** and **Approach 2**.

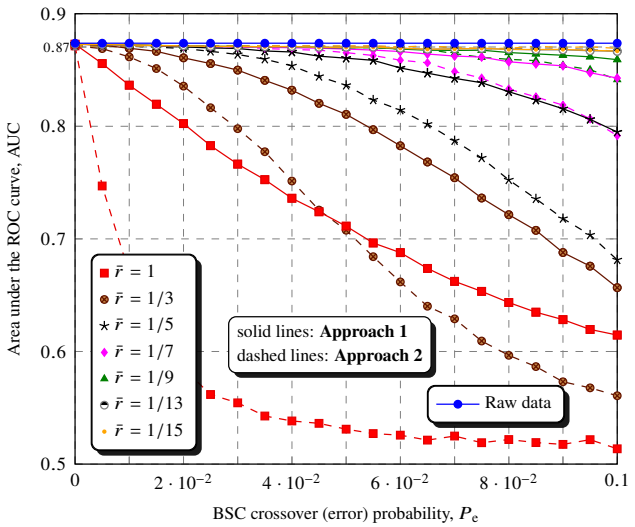

Fig. 4: AUC for the CF-CPSC as a function of P_e, with $b_1 = 5$ for the **Approach 1** and $b_2 = 6$ for the **Approach 2**, and variable code rates. This figure is better viewed in color.

without channel coding. A careful observation allows one to conclude that both approaches have approximately the same performances for $\bar{r} = 1/13$ and $\bar{r} = 1/15$, for any P_e. Additionally, their AUCs are approximately equal to 0.87, which is quite close to the raw data AUC. For the remaining coding rates, the larger sensitivity of the **Approach 2** is visible, especially for $\bar{r} = 1$ (no channel coding).

Up to this point, one may conclude that the **Approach 2** has to be definitely avoided due to its larger sensitivity to quantization and report channel errors. However, the **Approach 2** is considerably advantageous in terms of report data traffic, a consequence of having to report only the values of $r_{u,\ell}$ to the FC, and of requiring code rates not much smaller than those required by the **Approach 1**. This fact is an evidence about the importance of taking into account the report channel data traffic besides the spectrum sensing performance.

For the **Approach 1**, the amount of report channel bits depends on U, b_1, N, $\bar{r}$, as well as on the number of bits used to quantize ψ_u (which is 3), resulting in $U(2b_1N + 3)/\bar{r}$ bits in each sensing round, where the multiplier 2 accounts for the quantization of the real and the imaginary parts of $x_u(n)$.

In the case of **Approach 2**, the amount of report channel bits depends on U, b_2, L, and $\bar{r}$, resulting in $Ub_2L/\bar{r}$ bits in each sensing period, which is $(2b_1N + 3)/b_2L$ times smaller than in the **Approach 1** if the same coding rate is used for both. Table I synthesizes the above data traffics and their ratio.

TABLE I: CF-CPSC data traffics for the **Approach 1** and the **Approach 2**, and the ratio between these traffics.

CF-CPSC report channel data traffic.	
Approach 1	$U(2b_1N + 3)/\bar{r}$ bits
Approach 2	$Ub_2L/\bar{r}$ bits
Ratio	$(2b_1N + 3)/b_2L$

Using the simulation set up, it follows that $U(2b_1N+3)/\bar{r} = 6(2 \times 5 \times 160 + 3)/\bar{r} = 9618/\bar{r}$ for the **Approach 1**, and $Ub_2L/\bar{r} = 6 \times 6 \times 5/\bar{r} = 180/\bar{r}$ for the **Approach 2**, yielding the ratio $(2b_1N + 3)/b_2L = 9618/180 \approx 53.43$ if the same coding rate is used for both approaches. For instance, if $\bar{r} = 1$ for both, $U(2b_1N + 3)/\bar{r} = 9618$ and $Ub_2L/\bar{r} = 180$ bits.

Figure 5 depicts the data traffics for both approaches, as a function of the repetition code rate $\bar{r}$. It is clear the expressive superiority of the **Approach 2** over the **Approach 1**, in terms of report channel traffic. It can be seen that, even when the **Approach 2** makes use of the largest report channel resource (with $\bar{r} = 1/15$), the resultant traffic is $Ub_2L/\bar{r} = 2700$ bits. On the other hand, the smaller volume of data for the **Approach 1** is 9618 bits (with $\bar{r} = 1$), which means $9618/2700 \approx 3.5$ bits times more bits in the case of **Approach 1**. Besides, with $Ub_2L/\bar{r} = 2700$ bits, the **Approach 2** can satisfactory protect the report channel transmissions even with $P_e = 0.1$, which is a very high error probability.

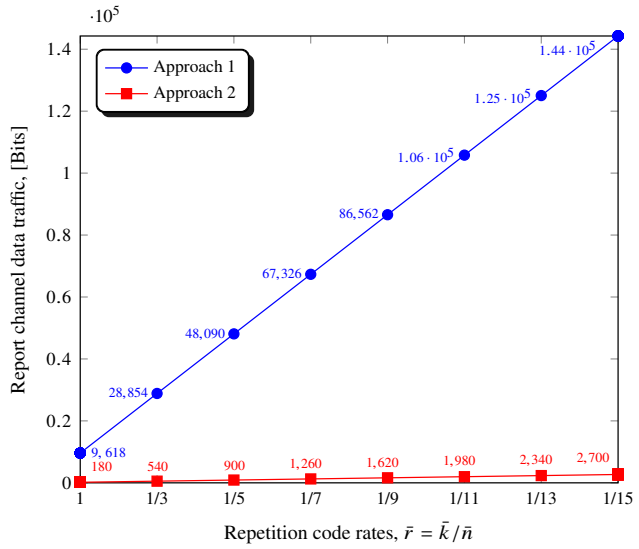

Fig. 5: Relation between the CF-CPSC report channel data traffics, in bits, and the code rate, $\bar{r}$, with $b_1 = 5$ bits for the **Approach 1**, and $b_2 = 6$ bits for the **Approach 2**.

Finally, notice that the difference between the data traffic produced by both approaches can be reduced or increased by changing N, L or both. For example, with fixed L the data traffic under the **Approach 1** can be reduced by reducing N. However, this unavoidably reduces the spectrum sensing performance as well, for the same SNR at the sensing channel (-10 dB in the present analysis). On the other hand, for a fixed N the data traffic achieved by the **Approach 2** is increased by increasing L, also reducing the spectrum sensing performance. For instance, with $N = 44$, the traffic of the **Approach 1**, without channel coding, becomes smaller than in the case of **Approach 2** with $\bar{r} = 1/15$, as can be calculated from Table I. However, from simulation results not presented here, due to the lack of space, this value of N drastically degraded the spectrum sensing performances for the adopted average SNR of -10 dB.

IV. Conclusions

This paper presented performance and report channel traffic analyses of the CF-CPSC algorithm for spectrum sensing under quantization and report channel errors. Repetition codes with a variety of coding rates were applied to protect the report channel transmissions, which were carried out through memoryless binary symmetric channel with configurable error probabilities.

Two approaches were investigated regarding the executions of the CF-CPSC algorithm. In **Approach 1** the algorithm was completely computed at the fusion center, and in **Approach 2** it was partially executed at the secondary terminals and finished at the fusion center, aiming at saving report channel resources.

Results showed that the CF-CPSC is robust under channel errors, considering the high error probabilities adopted for the analyses. Besides, results also showed that the **Approach 2** is more sensitive to quantization and report channel errors, but the amount of data at the report channel, even in the worst case, i.e., with repetition code and with the smallest code rate, is expressively smaller than for the **Approach 1** with the smallest amount of data, i.e., with no repetition code. The analysis revealed that the **Approach 2** is definitely the best choice for spectrum sensing with the CF-CPSC algorithm.

References

[1] J. G. Andrews, S. Buzzi, W. Choi, S. V. Hanly, A. Lozano, A. C. K. Soong, and J. C. Zhang, "What will 5G be?" *IEEE J. Sel. Areas Commun.*, vol. 32, no. 6, pp. 1065–1082, Jun. 2014.

[2] Y. Chen and H. S. Oh, "A survey of measurement-based spectrum occupancy modeling for cognitive radios," *IEEE Commun. Surveys Tuts.*, vol. 18, no. 1, pp. 848–859, Firstquarter 2016.

[3] T. Yucek and H. Arslan, "A survey of spectrum sensing algorithms for cognitive radio applications," *IEEE Commun. Surveys Tuts.*, vol. 11, no. 1, pp. 116–130, First 2009.

[4] H. Kour, R. K. Jha, and S. Jain, "A comprehensive survey on spectrum sharing: Architecture, energy efficiency and security issues," *J. of Network and Comput. Applicat.*, vol. 103, pp. 29 – 57, 2018.

[5] B. Nadler, F. Penna, and R. Garello, "Performance of eigenvalue-based signal detectors with known and unknown noise level," in *2011 IEEE Int. Conf. on Commun. (ICC)*, Jun. 2011, pp. 1–5.

[6] R. C. D. V. Bomfin, R. A. A. de Souza, and D. A. Guimarães, "Circular folding cooperative power spectral density split cancellation algorithm for spectrum sensing," *IEEE Commun. Lett.*, vol. 21, no. 2, pp. 250–253, Feb. 2017.

[7] A. Ghasemi and E. S. Sousa, "Collaborative spectrum sensing for opportunistic access in fading environments," in *First IEEE Int. Symp. on New Frontiers in Dynamic Spectrum Access Networks, 2005. DySPAN 2005.*, Nov. 2005, pp. 131–136.

[8] MathWorks. (2016, Dec.) PDF documentation for fixed-point designer. FPTUG.pdf.

[9] R. C. D. V. Bomfin and R. A. A. de Souza, "A new spatially correlated shadowed channel model with cognitive radio application," in *2015 IEEE 81st Veh. Tech. Conf. (VTC Spring)*, May 2015, pp. 1–5.

[10] *IEEE Standard for Information technology– Local and metropolitan area networks– Specific requirements– Part 22: Cognitive Wireless RAN Medium Access Control (MAC) and Physical Layer (PHY) specifications: Policies and procedures for operation in the TV Bands*, IEEE Std., Jul. 2011.